OPTIMIZATION OF ELLIPSOMETRIC COMPONENTS FOR USER FRIENDLY DETERMINATION OF OPTICAL PARAMETERS OF THIN FILMS

By

Sisay Mebre

SUBMITTED IN PARTIAL FULFILLMENT OF THE
REQUIREMENTS FOR THE DEGREE OF
MASTER OF SCIENCE
AT
ADDIS ABABA UNIVERSITY
ADDIS ABABA, ETHIOPIA
SEPTEMBER 2007

ADDIS ABABA UNIVERSITY
DEPARTMENT OF
PHYSICS

The undersigned hereby certify that they have read and recommend to the Faculty of Science for acceptance a thesis entitled "**Optimization of Ellipsometric Components for User Friendly Determination of Optical Parameters of Thin Films** " by **Sisay Mebre** in partial fulfillment of the requirements for the degree of **Master of Science**.

Dated: September 2007

Supervisors:

Dr. Araya Asfaw

Dr. Mesfin Redi

Examiner:

Dr. S K Ghoshal

Dr. Ahmed Mustefa

ADDIS ABABA UNIVERSITY

Date: **September 2007**

Author: **Sisay Mebre**

Title: **Optimization of Ellipsometric Components for User Friendly Determination of Optical Parameters of Thin Films**

Department: **Physics**

Degree: **M.Sc.** Convocation: **September** Year: **2007**

Signature of Author

TO My Grand Parents

(Assegid and Emamye)

Table of Contents

List of Tables

List of Figures

Abstract

In this work the optical constants and thickness of organic thin films is determined using ellipsometry technique. Because it is non-destructive and sensitive to several material characteristics, such as Layer thickness, optical constants (refractive index and extinction coefficient), Surface roughness Composition, Optical anisotropy. Choosing one of the number of ellipsometry setting rotating analyzer ellipsometry (RAE) techniques and by optimizing the components of the ellipsometery for automated way attempt was made to determine optical constants(complex and real refractive index),absorption and thickness of APFO-Green6 organic thin film which coated with a speed of 600rpm on glass substrate, for wavelengths 532nm, 632.8nm, 660nm, 808nm, 1064nm for five angle of incident to each wavelength.

Acknowledgements

I am very grateful to Dr. Araya Asfaw and Dr. Mesfin Redi, who inspired me to develop the habit of team work in research. I am specially grateful to Dr. Mesfin Redi for identification of the problem to be studied and his unreserved advise and suggestions almost in all parts of my experimental work. I can say that his suggestion and constructive criticism brought this paper to existence. I also thanks Dr. Wondemagegn Mamo,from Chemistry Department of Addis Ababa university for supplying the sample for the experiment. I also thank the polymer research group of Physics Department of Addis Ababa university for their help on preparing thin film. Further I would like to express my appreciation to Tesfaye Mamo, for his unreserved technical and supports on this work. Finally I would like to thank my uncle Dr.Habtamu Abie and all my friends who are on my side during this work,specially kusse Gudishe, Daniel Endeg, and Brihanu Beneberu for their unlimited help.

Sisay Mebre

September 25, 2007

Introduction

The ellipsometry technique has been discovered hundred years ago but it is only since the early 80's, thanks to the development of electronic and computers, that the technique expands largely in numerous fields. The strong advantages of ellipsometry are its non destructive character, its high sensitivity, its large measurement range (from fractions of single layers to micrometers), and the possibilities to control complex processes in real time.

An ellipsometer can be used to measure layers as thin as 1 nm up to layers which are several microns thick. Applications include the accurate thickness measurement of thin films, the identification of materials and thin layers and the characterization of surfaces.

There are two major kinds of widely used now a days these are ellipsometric spectroscopy(SE) and multiple angle of incident(MAI) ellipsometery. In SE, the reflection ratio is measured over a range of wavelength at a fixed angle of incident. But in MAI, the reflection ratio is measured over a range of wavelength at a variable angle of incident. We are interested here only on multiple angle of incident (MAI) ellipsometry to try to measure the refractive index and the thickness of semi-transparent thin films. The instrument relies on the fact that the reflection at a dielectric interface depends on the polarization of the light while the transmission of light through a transparent

layer changes the phase of the incoming wave depending on the refractive index of the material.

MAI, system generally employs laser source which are highly monochromatic and have higher intensity at a specific wavelength that ordinary light source. The setup is rotating analyzer ellipsometry. The reflected light is analyzed by rotating analyzer for five wave length at five different incident angles for each wavelength.

The material (sample) we use for our work is APFO-green6 which uses for plastic solar cell and production of photovoltaic cells

Chapter 1

Light and Matter

1.1 Nature of Light

Without light, life as we know it would not exist. Plants harvest solar energy by photosynthesis, and provide energy to other organisms through the food chain. We human beings and animals depend on light through vision and other photoresponses. Biological effects of artificial light are the basis of a variety of medical treatments and diagnostic techniques. Because of its potential of carrying information, it also uses for distance research and communication. In general light is everywhere in our world. As a result scientists began to ask what light realy is? Speculation about the true nature of of light go by centuries. Pythagorean believed that light consists of a minute particles shoot out at high speed from luminous object. Plato and his co-thinker regarded light as some kinds of emanations from the eye by means of which objects are scanned and made visible when struck by it. Aristotle thought light is something non materials according to the space intervening the eye and the object examined[1]. The rectilinear propagation of light, as well as law of reflection, was explained by Euclid in 300BC [2].

The evolution in our understanding of the physical nature of light forms one of the most fascinating accounts in the history of science. Since the dawn of modern science in the sixteenth and seventeenth centuries, light has been pictured either as particle or wave. In the twentieth century it became clear that somewhat light was both wave and particle, yet it was precisely neither. This concept refereed to as the wave-particle duality. The solution was achieved through the creation of quantum electrodynamics, one of the most successful theoretical structures in the annals of physics [2].

In the seventeenth century Issac Newton presented the most outstanding theory of a particle nature of light. According to his theory, light consists of a streams of minute invisible particles, called corpuscules, emitted from a source of light and traveling in straight lines with a great speed.

In 1690, Christian Huygens, a Dutch scientist in contrary to Newton, presented the wave theory. In his treatise of light that beam of light consists of a large number of longitudinal pulse which spreading out from a light source in all directions and propagating through an all-pervasive elastic medium called the ether. Twelve years after the presentation of his wave theory, Huygens was successful in explaining reflection and refraction and to explain double refraction in calcite as well [1].

Within two years of the century of the publication of Newton's Optics, the Englishman Thomas Young performed a decisive experiment that seemed to demand a wave theory of light. It was the double-slit experiment, in which an opaque screen with two small, closely spaced openings was illuminated by monochromatic light from a small source. The "shadows" observed formed a complex interference pattern like those produced with water waves [1].

Victories for the wave theory continued up to the twentieth century. In the mood of scientific confidence that characterized the latter part of nineteenth century, there was little doubt that light, like most other classical areas of physics, was well understood.

In 1821 Augustin Fresnel published results of his experiments and analysis, which required that light be a transverse wave. On this basis, double refraction in calcite could be understood as a phenomenon involving polarized light. It had been assumed that light wave in an ether were necessary longitudinal, like sound weaves in a fluid, which can't support transverse vibrations. For each of two components of polarized light, Fresnel developed the Fresnel equations which give the amplitude of reflected and transmitted light at a plane of interface separating two optical media [1].

In 1873, working in the field of electricity and magnetism, James Clerk Maxwell synthesized the well known principles in his set of four Maxwell equations [1]. The equations yield a prediction for the speed of an electromagnetic wave in the ether that turned out to be the measured speed of light, suggesting its electromagnetic character. From then on, light was viewed as a particular region of the electromagnetic spectrum of radiation. The experiment (1887) of Albert Michelson and Edward Morley, which attempted to detect optically the earth's motion through the ether, and the theory of relativity (1905) of Albert Einstein were of high importance. Together they led inevitably to the conclusion that the assumption of an ether was superfluous. The problem associated with transverse vibrations of a wave in a fluid thus vanished. In 1900, Max Plank announced at a meeting of the German Physical Society that he was able to derive the correct black body radiation spectrum only by making the curious assumption that atoms emitted light in discrete energy (quanta) rather than in a continuous manner. Plank's quantum hypothesis, which constitute a clear

break with the doctrine of classical physics, along with Einstein's idea of photons charactor of light constitute what is now called Quantum theory of light. Another striking confirmation of the photon character of light is provided by the interpretation of emission and absorption of line spectra in 1913 by Neils Bohr and compton's experimental observation and interpretation. In 1924 Luis de Broglie presented his speculations that sub atomic particles are endowed with wave particles. Thus the wave-particle duality came full circle. Light behaved like waves in its propagation and in the phenomena of interference reflection, refraction, diffraction and polarization; it would, however, also behave as particles in its interaction with matter (photo-electric-effect) and in the process of absorption, emission and scattering)[1].

1.2 Maxwell's and Electromagnetic Wave Equations

Working in the field of electricity and magnetism, James Clerk Maxwell shows that light behaves like an electromagnetic waves, i.e a propagating disturbance involving time and space variation of the coupled electric and magnetic fields.

In general the propagation of light through a medium can best be understood in terms of electromagnetic waves, therefore, the behavior of electric field $\overrightarrow{E}$ and magnetic field $\overrightarrow{B}$ which are independent of one another can be described by the wonderful and beautiful Maxwell equations. Some of which relate $\overrightarrow{E}$ and $\overrightarrow{B}$ to the charge density (ρ) and current density (J) respectively

For neutral dielectric medium (one with no free charge) or for free space the Maxwell equation are

$$\overrightarrow{\nabla} \cdot \overrightarrow{D} = 0 \tag{1.2.1}$$

$$\overrightarrow{\nabla} \cdot \overrightarrow{B} = 0 \tag{1.2.2}$$

$$\overrightarrow{\nabla} \times \overrightarrow{E} = -\frac{\partial \overrightarrow{B}}{\partial t} \tag{1.2.3}$$

$$\overrightarrow{\nabla} \times \overrightarrow{B} = \mu_0(\frac{\partial \overrightarrow{D}}{\partial t} + \overrightarrow{J}) \tag{1.2.4}$$

Where $\overrightarrow{D}$ is electric displacement vector. Here we will be interested only non-magmatic media for which

$$\overrightarrow{B} = \mu_0 \overrightarrow{H} \tag{1.2.5}$$

The electric displacement vector $\overrightarrow{D}$ is defined as

$$\overrightarrow{D} = \varepsilon_0 E + \overrightarrow{P} \tag{1.2.6}$$

Where $\overrightarrow{P}$ is the polarization which is the electric dipole moment per unit volume of the medium. $\overrightarrow{P}$ is the only term in the Maxwell equation related to the medium

Now if we substitute equation (1.2.5) and equation (1.2.6) into equation (1.2.1) to (1.2.4) the Maxwell equation can be written as

$$\overrightarrow{\nabla} \cdot \overrightarrow{E} = -\frac{1}{\varepsilon_0} \overrightarrow{\nabla} \cdot \overrightarrow{P} \tag{1.2.7}$$

$$\overrightarrow{\nabla} \cdot \overrightarrow{H} = 0 \tag{1.2.8}$$

$$\overrightarrow{\nabla} \times \overrightarrow{E} = -\mu_0(\frac{\partial \overrightarrow{H}}{\partial t}) \tag{1.2.9}$$

$$\overrightarrow{\nabla} \times \overrightarrow{H} = \varepsilon_0 \frac{\partial \overrightarrow{E}}{\partial t} + \frac{\partial \overrightarrow{\rho}}{\partial t} + \overrightarrow{J} \tag{1.2.10}$$

Now we are free to derive the general wave equation of for the electric field. To do so first let us take the curl of equation (1.2.9) and substituting (1.2.10) to eliminate

the magnetic field $\overrightarrow{H}$, i.e

$$\overrightarrow{\nabla} \times (\overrightarrow{\nabla} \times \overrightarrow{E}) + \frac{1}{c^2}\frac{\partial^2 \overrightarrow{E}}{\partial t^2} = -\mu_0(\frac{\partial^2 \overrightarrow{\rho}}{\partial t^2} + \frac{\partial \overrightarrow{J}}{\partial t}) \tag{1.2.11}$$

The two terms on the right hand side of equation (1.2.11) are called source terms. They stem from the presence of polarization charge and conduction charge respectively, within the medium. It is also possible to find the general wave equation for magnetic field $\overrightarrow{H}$ by taking the curl of equation (1.2.9) and substituting (1.2.10) to eliminate the electric field [4, 5].

1.3 Reflection and Refraction of Light at the Plane boundary

To study the reflection and transmission of light at the interface of the two media let us consider a plane wave incident upon a plane boundary separating two different semi-infinite homogeneous optically isotropic media

The wave incident from medium 0 with an angle θ_0 from the normal to the interface gives to reflected wave in the some medium and transmitted (refracted) wave in medium 1 with an angle θ_1 from the normal. The complex forms of the plane harmonic wave is given as

$$\overrightarrow{E} = \hat{E_0} \exp -i(\omega t - \overrightarrow{k} \cdot \overrightarrow{r}) \tag{1.3.1}$$

$$\overrightarrow{B} = \hat{B_0} \exp -i(\omega t - \overrightarrow{k} \cdot \overrightarrow{r}) \tag{1.3.2}$$

Where $\hat{E_0}$ and $\hat{B_0}$ are complex vector amplitude which are independent of $\overrightarrow{r}$ and t.

The total field inside media 0 and 1 must obey Maxwell's equations and boundary condition. For a given amplitude and polarization of incident wave, the amplitude and

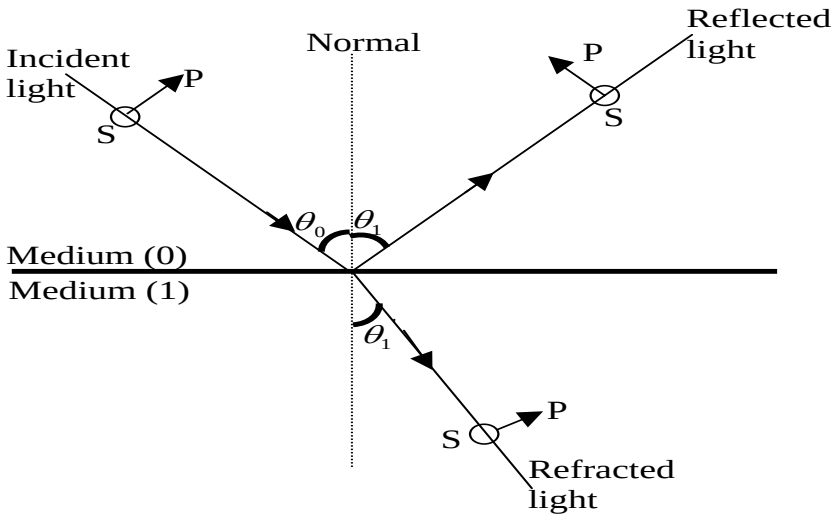

Figure 1.1: Reflction and refraction of light at the plane boundary .

polarization of reflected and transmitted waves can be determined from the continuity of the tangential components of the electric and magnetic field vectors across the interface between the two isotropic media. The incident electric field $\overrightarrow{E}$ can be decomposed into two orthogonal components. The component perpendicular to the plane of incident is s-component and the component parallel to the plane of incident is p-component.

From the boundary condition, the fresnel equation (the coefficients of reflection r_s and r_p and the coefficients of transmission t_s and t_p, which are defined as the amplitude ratio) for s- and p-polarization can be derived.

$$r_s = \frac{E'_{0s}}{E_{os}} = \frac{n_o \cos\theta_0 - n_1 \cos\theta_1}{n_o \cos\theta_0 + n_1 \cos\theta_1} \tag{1.3.3}$$

$$r_p = \frac{E'_{0p}}{E_{op}} = \frac{n_1 \cos\theta_0 - n_1 \cos\theta_1}{n_1 \cos\theta_0 + n_0 \cos\theta_1} \tag{1.3.4}$$

$$t_s = \frac{E'_{1s}}{E_{os}} = \frac{2n_o \cos\theta_0}{n_o \cos\theta_0 + n_1 \cos\theta_1} \tag{1.3.5}$$

$$t_p = \frac{E'_{0s}}{E_{op}} = \frac{2n_o \cos\theta_0}{n_o \cos\theta_0 + n_1 \cos\theta_1} \tag{1.3.6}$$

The snell's law of the this system (for the two media) is given as

$$n_0 \sin\theta_0 = n_1 \sin\theta_1 \tag{1.3.7}$$

When p-polarized light wave is incident on the the transparent media, the reflection wave will be zero at a particular incident angle θ. The incident is totally refracted to the second medium, such that setting $r_p = 0$ and using snell's law we can get

$$\theta = \tan^{-1}(\frac{n_1}{n_0}) \tag{1.3.8}$$

This angle is called the polarizing angle or Brewster angle. It is a function of wavelength because of dispersion. The variation over the visible spectrum is very small[5].

1.4 Polarization

Polarization is a property that is common to all types of vector waves. Electromagnetic waves possess this property, as a result, electromagnetic wave theory of light is used to explain polarization phenomenon. There are three types of polarized light, plane (linear), elliptical and circular polarized light. When light interact with matter, the force exerted on the the electron by the electric field of light is much greater than the magnetic field. that is why the polarization is determined by the direction of electric field. Because the electric field is a vector quantity we must specify both its magnitude and direction. Consider a monochromatic plane wave of angular frequency ω and wave vector k, parallel to the z-axis. In an infinite medium and in the case of

homogeneous plane waves, two orthogonal electric field vector can represent the light wave:

$$E_x = iA_x \cos(kz - \omega t - \phi_x) \tag{1.4.1}$$

$$E_y = jA_y \cos(kz - \omega t - \phi_y) \tag{1.4.2}$$

where A_x and A_x are amplitude of the waves ϕ_x and ϕ_y are orthogonal components of the phase of the waves, i and j are unit base vector in cartesian coordinates. The phase difference between the two orthogonal component is given as $\delta = \phi_y - \phi_x$

The total electric field $\overrightarrow{E}$ is the vector sum of the two component fields.

$$\overrightarrow{E} = iA_x \cos(kz - \omega t - \phi_x) + jA_y \cos(kz - \omega t - \phi_y) \tag{1.4.3}$$

For simplicity let $\phi_x = 0$ as a result $\delta = \phi_y$, then the equation (1.4.1) to (1.4.3) become

$$E_x = iA_x \cos(kz - \omega t) \tag{1.4.4}$$

$$E_y = jA_y \cos(kz - \omega t - \delta) \tag{1.4.5}$$

$$\overrightarrow{E} = iA_x \cos(kz - \omega t) + jA_y \cos(kz - \omega t - \delta) \tag{1.4.6}$$

The state of polarization of light is described by the so called the polarization ellipse, which can be observe by following the extremity of the $\overrightarrow{E}$ vector in the wave plane. We can deduce the equation of this ellipse from equation (1.4.4) to (1.4.6):

$$(\frac{E_x}{A_x})^2 + (\frac{E_y}{A_y})^2 - \frac{2E_xE_y \cos\delta}{A_xA_y} = \sin^2\delta \tag{1.4.7}$$

This equation is the combination of two electric fields that are mutually perpendicular to each other and differing in phase by an angle δ , and represents an elliptical polarization of light. The classification of the types of polarized light will depend on

the relative phase δ, and the relative sizes of A_x and A_y. The sign δ determine the sense of rotation

Case I When $\delta = 0$ or $\delta = \pi$ or an integral multiple of π, equation (1.4.7) become

$$E_y = \pm \frac{A_y}{A_x} E_x \tag{1.4.8}$$

These shows the light is linearly polarized. The electric field undergoes simple harmonic motion along a line $y = \pm \frac{A_y}{A_x} x$.

Case II When $\delta = 0$ or $\delta = \pm \frac{\pi}{2}$ or an integral multiple of $\pm \frac{\pi}{2}$, and $A_x = A_y = A$, equation (1.4.7) become

$$(E_x)^2 + (E_Y)^2 = A^2 \tag{1.4.9}$$

This is the equation of circle , that means the light is circularly polarized. A given vector process with a constant angular speed and with constant magnitude. If the x-component of electric field leads the y-component, we have a clockwise rotation and the light is said to be circular polarized.

Case III When $A_x \neq A_y$, the equation is ellipse that means the light is elliptically polarized

Case IV For the general case, when δ is not an integral multiple of π and $\frac{\pi}{2}$, we will have elliptical polarized light whose major and minor Axis does not lie along x-and y-axis. The tilting angle ϕ is defined as

$$\tan \phi = \frac{2ab \cos \phi}{a^2 - b^2}$$

where b is semi-minor axis and a is semi-major axis. Ellipticity e is the ratio of the length of semi-minor (b) and semi-major (a) axis of the ellipse. The right and left handed circularly polarized light corresponds to $e = 1$ and $e = -1$ respectively. Linearly polarized light have ellipticity of zero magnitude [6].

1.4.1 Stokes Parameters

Stokes parameters, an alternative representation of the state of polarization of light, are all real numbers and measurable. Stokes parameters consists of four real numbers, directly related to the intensity of light [13]:

$$S_0 = E_x E_x^* + E_x E_y^* = I_x + I_y \tag{1.4.10}$$

$$S_1 = E_x E_x^* - E_x E_y^* = I_x - I_y \tag{1.4.11}$$

$$S_2 = E_x E_y^* + E_y E_x^* = I_{45^0} - I_{-45^0} \tag{1.4.12}$$

$$S_3 = i(E_x E_y^* + E_y E_x^* = I_{RCP} - I_{LCP} \tag{1.4.13}$$

The Stokes parameters of monochromatic light wave can be grouped in a 4×1 column vector [8]:

$$S = \begin{pmatrix} S_0 \\ S_1 \\ S_2 \\ S_3 \end{pmatrix} \tag{1.4.14}$$

called the Stokes vector of the wave. This can also be written horizontally between curly brackets and the elements separated by commas as follows

$$S = \{S_0, S_1, S_2, S_3\} \tag{1.4.15}$$

We observe that for unpolarized light, there is no preference to any particular polarizations so that $S_1 = S_2 = S_3 = 0$ and the Stokes vector assumes the form

$$S_{un} = \{S_0, 0, 0, 0\} \tag{1.4.16}$$

Generally the polarized light satisfies the following condition

$$S_0^2 = S_1^2 + S_2^2 + S_3^2 \tag{1.4.17}$$

since the stokes parameters S_0, S_1, S_2 and S_3 are measurable quantities. Thus, the measure of these intensities allows the unambiguous determination of the state of polarization of light. This is the basic principle behind many ellipsometers.

The physical meaning of stokes parameters is particularly important in the study of partially polarized light, in which the notion of the phase difference between components does not have much of a meaning. From the definition, none of the parameters can be greater than S_0, which is usually normalized to 1. for completely polarized light, we have:

$$S_1^2 + S_2^2 + S_3^2 = 1 \tag{1.4.18}$$

while for entirely unpolarized light:

$$S_1^2 + S_2^2 + S_3^2 = 0 \tag{1.4.19}$$

and partially polarized and unpolarized light satisfies the inequality

$$S_0^2 > S_1^2 + S_2^2 + S_3^2 \tag{1.4.20}$$

The degree of polarization is therefore defined as:

$$p = \frac{\sqrt{S_1 + S_2 + S_3}}{S_o} \tag{1.4.21}$$

The degree of polarization p varies from zero for unpolarized light to unity in the case of totally polarized light and assumes intermediate (fraction) values for partially polarized light.

1.4.2 Poincare Sphere

For completely polarized light the relation of equation (1.3.8) always holds, so we can view the parameters $(S_1, S_{2,}S_3)$ as the coordinates of a point on the unit sphere

called the poincaré sphere. On the poincare sphere each point represents a specific polarization state. The point on the equator represents linearly polarized state. The left and right circularly polarized states are represented by the south and north poles respectively. points on the lower and upper hemisphere represents the degree of left and right elliptically polarized states, respectively. Any pairs of antipodal point on the poincare sphere corresponds to states with orthogonal polarization.Excluding the origin, any point inside the unit sphere, $0 < p < 1$, represents a partially polarized light. Points outside the unit sphere, $p > 1$, don't represent any physical state of polarization.

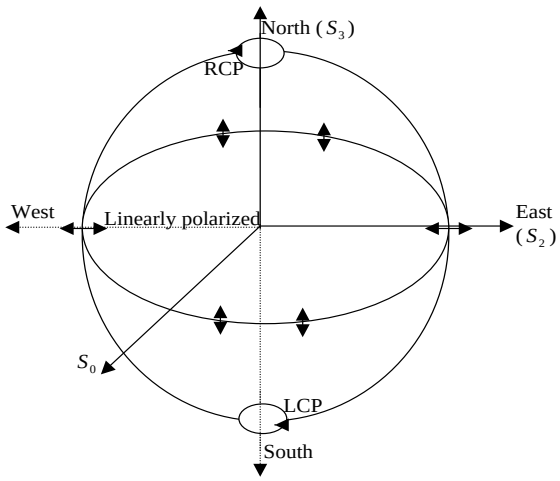

Figure 1.2: Polarization state representation of light using poincare sphere.

This representation is particularly useful to describe the polarization transformation through an anisotropic medium. For example, to visualize the evolution of the state of polarization when light passes through a linear birefringent plate as a curve on the poincare sphere.

1.5 Jones Vector and Matrix

In ellipsometery there are a sequence of elements and each of each modifies the state of polarization in specific manner. R. Clark Jones fifty years ago used a very useful technique for describing the change in polarization state of the light as it passed through an optical system containing various interfaces and polarizing elements. Jones treats the optical system as a linear system describable by an appropriate Jones matrix that transforms vectors describing the polarization state of the wave. In a linear system description the output Jones vector of a light wave after it has interacted with an optical system has components that are linearly related to its input components. The types of optical devices that can be so represented include linear polarizers, circular polarizers, phase retarders and isotropic phase changers.

The electric field of a light wave linearly polarized along the x- and y-axis is written in the exponential form as

$$E_x = A_x \exp i(\omega t + \phi_x) = A_x \exp i(\omega t) \exp i(\phi_x) \tag{1.5.1}$$

$$E_y = A_y \exp i(\omega t + \phi_y) = A_y \exp i(\omega t) \exp i(\phi_y) \tag{1.5.2}$$

where A_x and A_y are amplitude of the fields. The superposition of the two electric fields E_x and E_y leads in to general elliptically polarized light with electric field

$$E = [A_x \exp i(\phi_x) + A_y \exp i(\phi_y)] \exp i(\omega t) \tag{1.5.3}$$

The complex amplitude of the x- and y-components of this wave form a two elements of Jones vectors, where

$$J = \begin{pmatrix} E_x \\ E_y \end{pmatrix} = \begin{pmatrix} A_x \exp(i\phi_x) \\ A_y \exp(i\phi_y) \end{pmatrix} \tag{1.5.4}$$

clearly, linearly polarized light along x-and y-axis are

$$J = \begin{pmatrix} A_x \exp(i\phi_x) \\ 0 \end{pmatrix} \qquad and \qquad J = \begin{pmatrix} 0 \\ A_y \exp(i\phi_y) \end{pmatrix} \tag{1.5.5}$$

respectively.In general linearly polarized light with at angle β with the axis has

$$J_\beta = \begin{pmatrix} E_o \cos\beta \\ E_0 \sin\beta \end{pmatrix} \tag{1.5.6}$$

Right and left handed circularly polarized light has

$$J_{rcp} = \begin{pmatrix} E_0 \exp(i\phi_x) \\ E_0 \exp i(\phi_x + \frac{\pi}{2}) \end{pmatrix} \qquad and \qquad J_{lcp} = \begin{pmatrix} E_0 \exp(i\phi_x) \\ E_0 \exp i(\phi_x - \frac{\pi}{2}) \end{pmatrix} \tag{1.5.7}$$

respectively. In linear system description the output Jones vector of a light wave after it has interacted with an optical system has a components that are linearly related to its input components. If

$$J_{in} = E_x i + E_y j \qquad and \qquad J_{out} = E_x^{'} i + E_y^{'} j \tag{1.5.8}$$

Where phase factor included in the complex amplitudes, we can now write

$$E_x^{'} = m_{11}E_x + m_{12}E_y$$

$$E_y^{'} = m_{21}E_x + m_{22}E_y$$

or in matrix form

$$\begin{pmatrix} E_x^{'} \\ E_y^{'} \end{pmatrix} = \begin{pmatrix} m_{11} & m_{12} \\ m_{21} & m_{22} \end{pmatrix} \begin{pmatrix} E_x \\ E_y \end{pmatrix} \tag{1.5.9}$$

Equation (1.5.9) introduces the Jones matrix M with elements m_{ij}, it can be written as

$$J_{out} = M J_{in} \tag{1.5.10}$$

Optical Device	**Jones Matrix**
Linearly polarizer oriented along $x-$*direction*	$\begin{pmatrix} 1 & 0 \\ 0 & 0 \end{pmatrix}$
Linearly polarizer oriented along $y-$*axis*	$\begin{pmatrix} 0 & 0 \\ 0 & 1 \end{pmatrix}$
Linearly polarizer oriented at an angle θ *to the* $x-$*axis*	$\begin{pmatrix} \cos^2\theta & \sin\theta\cos\theta \\ \sin\theta\cos\theta & \sin^2\theta \end{pmatrix}$
Right circular polarizer	$\frac{1}{2}\begin{pmatrix} 1 & i \\ -i & 1 \end{pmatrix}$
$Left$ *circular polarizer*	$\frac{1}{2}\begin{pmatrix} 1 & -i \\ i & 1 \end{pmatrix}$
$Quarter-wave\ plate,\ fast\ axis\ horizontal$	$\exp(\frac{i\pi}{4})\begin{pmatrix} 1 & 0 \\ 0 & i \end{pmatrix}$
$Quarter-wave\ plat,\ fast\ axis\ vertical$	$\exp(\frac{i\pi}{4})\begin{pmatrix} 1 & 0 \\ 0 & -i \end{pmatrix}$

Table 1.1: Jones matrix for common optical devices.

The determination of the Jones matrix for a common optical elements is straight forward. It should be noticed that the Jones vector is of use only for computing results with light that is initially polarized in some way, that means, there is no Jones vector representation for unpolarized light [5]

1.5.1 Mueller Matrix

The Mueller calculus is useful for coherent, partially coherent and incoherent light. In this calculus, the Mueller matrices represent optical elements that operate on Stokes vectors that represent lights with various states of polarization. The Mueller matrices represents the action of an optical elements on on the polarization states of light that is described as a stokes vectors.

$$\overrightarrow{S}_{out} = \overline{M}\,\overrightarrow{S}_{in} \tag{1.5.11}$$

where M is 4×4 matric [7].

Optical component	Mueller matrix
1. A perfect linear polarizer with horizontal transmission axis	$\frac{1}{2}\begin{bmatrix} 1 & 1 & 0 & 0 \\ 1 & 1 & 0 & 0 \\ 0 & 0 & 0 & 0 \\ 0 & 0 & 0 & 0 \end{bmatrix}$
2. A partial linear polarizer with horizontal transmission axis and attenuation coefficient α	$\frac{1}{2}\begin{bmatrix} 1+\alpha & 1-\alpha & 0 & 0 \\ 1-\alpha & 1+\alpha & 0 & 0 \\ 0 & 0 & 2\sqrt{\alpha} & 0 \\ 0 & 0 & 0 & 2\sqrt{\alpha} \end{bmatrix}$
3. Ellipsomertic reflection sample where the major axis is determined by the plane of incidence	$\begin{bmatrix} 1 & -\cos 2\Psi & 0 & 0 \\ -\cos 2\Psi & 1 & 0 & 0 \\ 0 & 0 & \sin 2\Psi \cos\Delta & \sin 2\Psi \sin\Delta \\ 0 & 0 & -\sin 2\Psi \sin\Delta & \sin 2\Psi \cos\Delta \end{bmatrix}$
4. A matrix to represent a component in another fame of reference rotated over angle θ relative to the old frame of reference.	$\frac{1}{2}\begin{bmatrix} 1 & 0 & 0 & 0 \\ 0 & \cos 2\theta & \sin 2\theta & 0 \\ 0 & -\sin 2\theta & \cos 2\theta & 0 \\ 0 & 0 & 0 & 1 \end{bmatrix}$

Table 1.2: Mueller matrices of some optical components.

Chapter 2

Ellipsometry

2.1 Introduction

Ellipsometry is an optical technique devoted to the analysis of the states of polarization of polarized vector waves, and conducted to obtained characteristics information about an optical system that modifies the state of polarization. This change of states of polarization can be related to the initial state and the optical properties of optical systems under investigation. The optical system acts as a transformation matrix, which can be handle by Jones and Mueller matrices under different circumstances, that changes the initial state to the final one. The optical systems can modifies the states of polarization of light through reflection, refraction , transmission, scattering or a combination of these. Based on these ellipsometry deals with the reflection experiments (reflection or surface ellipsometry) which will be discussed on this paper, transmission experiment (polarimetry) and scattering experiments (scattering ellipsometry). The ellipsometry technique has been discovered a century ago but it is only since the early 80's, thanks to the development of electronics and computers that the

technique expands largely in numerous fields. The strong advantages of ellipsometry are its non destructive character, its high sensitivity due to the measurement of the phase of the reflected light, its large measurement range (from fractions of single layers to micrometers), and the possibilities to control complex processes in real time. We must distinguish between single wavelength ellipsometry which can measure only two parameters and spectroscopic ellipsometry which can analyze complex structures such as multilayers, interface roughness, inhomogeneous layers, anisotropic layers and much more [8, 9]. We are interested here only by Spectroscopic Ellipsometry.

Nowadays ellipsometry has a wide ranges of application. Among the many useful application in optics for the measurement of optical properties of materials and their frequency dependance(wavelength dispersion). It is used in chemistry for analytical method and in electrochemistry for the characterization of the electrified interface in the presence of a surface film [8] It is also used in metrology to study haze, clouds and rain. It has also vast application in Biology, Astrology and medicine.

2.2 Theory of Ellipsometry

Ellipsometry measures two values, Ψ and Δ, which are related to the polarization change of the light caused by its interaction with a sample. These two values by themselves aren't very useful in characterizing a sample. What we really want to know are things like film thickness, optical constants, refractive index, and other useful data. These characteristics are found by using the measured values, Ψ and Δ, in various equations and algorithms to produce a model that describes the interaction of light with the sample. After reflection on a sample surface, a linearly polarized light beam is generally elliptically polarized. The reflected light has phase changes that

are different for electric field components polarized parallel (p) and perpendicular (s) to the plane of incidence. Ellipsometry measure this state of polarization or more precisely the complex ratio ρ written as:

$$\rho = \frac{r_p}{r_s} = \tan\Psi \exp i\Delta \tag{2.2.1}$$

where Ψ and Δ are the amplitude ratio and phase shift, respectively, of the p and s components. The reflectance coefficients are directly related to the optical constants of the surface by assuming the ambient is air of refractive index $n_0 = 1$ (Fresnel relations):

$$r_p = \frac{n\cos\phi_0 - \cos\phi_1}{n\cos\phi_0 + \cos\phi_1} \qquad r_s = \frac{\cos\phi_0 - n\cos\phi_1}{\cos\phi_0 + n\cos\phi_1} \tag{2.2.2}$$

where n is the complex refractive index of the surface.

2.3 Reflection and Transmission By Ambient-Film-Substrate System

Consider the film medium (1) that has a parallel plane boundaries of separation (film thickness)d and sandwiched between semi-infinite ambient (medium 0) and substrate (medium 2) as shown in the figure All ambient, film and substrate are homogeneous and optically isotropic with a complex refractive index n_0, n_1 and n_2 respectively. If the medium of incident is transparent n_0 is real

Now consider a plane electromagnetic waves incident in the medium 0 at an angle ϕ_0 will partially reflected and partially refracted (transmitted) to the second medium (film). Considering the s-components of the incident light the reflected wave will be s-component. The refracted wave inside the film suffers a multiple reflection at the

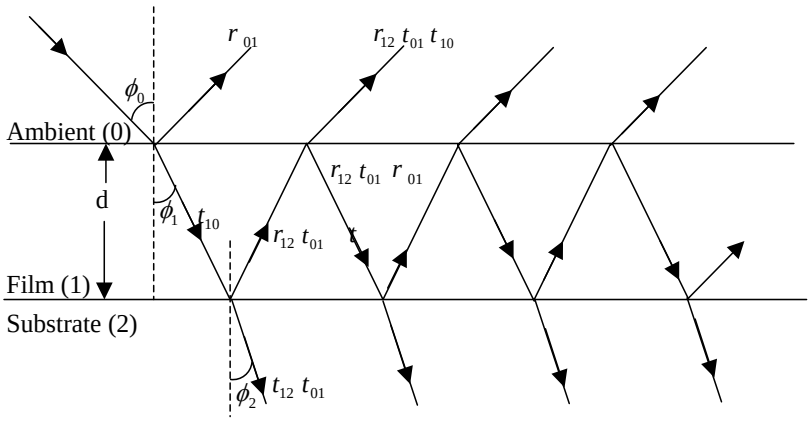

Figure 2.1: Reflection and transmission of light at a typical three-layer system (air-film-substrate). The amplitude of some of the reflected and transmitted beams is shown.

interfaces of 1-2 and 1-0 of the film boundaries, which are generally not perfectly reflecting. If the fresnel reflection and transmission coefficients of the interface $1-0$ $(0-1)$ and $1-2$ are denoted by r_{10s} t_{10s} $(r_{01s}$ $t_{01s})$ and r_{12s} t_{12s} respectively.The complex amplitude of the successive partial plane waves that makes the resultant reflected waves in medium 0 an d transmitted in medium 2 are r_{01s}, $t_{01s}t_{10s}r_{12s}\exp -i2\beta$, $t_{01s}t_{10s}r_{12s}r_{10s}\exp -i4\beta$,... and $t_{10s}t_{12s}\exp -i\beta$, $t_{10s}t_{12s}r_{10s}r_{12s}\exp -i3\beta$,... respectively. where β is the phase angle (film phase thickness) is given by

$$\beta = \frac{2\pi d n_1 \cos\phi_1}{\lambda} \tag{2.3.1}$$

Addition of the partial wave leads to infinite infinite geometric series for the total reflected amplitude R , which is given by

$$R = r_{01s}+t_{01s}t_{10s}r_{12s}\exp -i2\beta+t_{01s}t_{10s}r_{12s}r_{10s}\exp -i4\beta+t_{01s}t_{10s}r_{10s}^2 r_{12s}^3\exp -i6\beta+... \tag{2.3.2}$$

After summing the infinite geometric series and using the relation $r_{10s} = -r_{01s}$ and $t_{10s}t_{01s} = 1 - r_{10s}^2$, the result became

$$R_s = \frac{r_{01s} + r_{12s} \exp -i2\beta}{1 + r_{01s}r_{12s} \exp -i2\beta} \tag{2.3.3}$$

similarly for p-component

$$R_p = \frac{r_{01p} + r_{12p} \exp -i2\beta}{1 + r_{01p}r_{12p} \exp -i2\beta} \tag{2.3.4}$$

and like wise the total transmitted amplitude T is given by infinite geometric series

$$T_s = t_{10s}t_{12s} \exp -i\beta + t_{10s}t_{12s}r_{10s}r_{12s} \exp -i3\beta + ... \tag{2.3.5}$$

whose summation yields

$$T_s = \frac{t_{01s}t_{12s} \exp -i\beta}{1 + r_{01s}r_{12s} \exp -i2\beta} \tag{2.3.6}$$

Similarly for the p-component is

$$T_p = \frac{t_{01p}t_{12p} \exp -i\beta}{1 + r_{01p}r_{12s} \exp -i2\beta} \tag{2.3.7}$$

Where β is the same for both P- and S-components of polarization which is given by equation (2.3.1).

The fresnel reflection and transmission coefficients at the interface $0-1$ and $1-2$ are given by

$$r_{01p} = \frac{n_1 \cos\phi_0 - n_0 \cos\phi_1}{n_1 \cos\phi_0 + n_0 \cos\phi_1} \tag{2.3.8}$$

$$r_{01s} = \frac{n_0 \cos\phi_0 - n_1 \cos\phi_1}{n_0 \cos\phi_0 + n_1 \cos\phi_1} \tag{2.3.9}$$

$$r_{12p} = \frac{n_2 \cos\phi_1 - n_1 \cos\phi_2}{n_2 \cos\phi_1 + n_1 \cos\phi_2} \tag{2.3.10}$$

$$r_{12s} = \frac{n_1 \cos\phi_1 - n_2 \cos\phi_2}{n_1 \cos\phi_1 + n_2 \cos\phi_2} \tag{2.3.11}$$

$$t_{01p} = \frac{2n_0 \cos\phi_0}{n_1 \cos\phi_0 + n_0 \cos\phi_1} \tag{2.3.12}$$

$$t_{01s} = \frac{2n_0 \cos\phi_0}{n_0 \cos\phi_0 + n_1 \cos\phi_1} \tag{2.3.13}$$

$$t_{12p} = \frac{2n_1 \cos\phi_1}{n_2 \cos\phi_1 + n_1 \cos\phi_2} \tag{2.3.14}$$

$$t_{12s} = \frac{2n_1 \cos\phi_1}{n_1 \cos\phi_1 + n_2 \cos\phi_2} \tag{2.3.15}$$

The three angles are ϕ_0 ϕ_1 and ϕ_2 are related by snell's law

$$n_0 \sin\phi_0 = n_1 \sin\phi_1 = n_2 \sin\phi_2 \tag{2.3.16}$$

To apply the above theory to practical film substrate system, the following condition has to to be fulfilled [14]

1. The lateral dimension of the film must be many many times its thickness.

2. The source's bandwidth, beam diameter and degree of collimation as well as film thickness must be such that the multiple reflected and transmitted waves combined coherently.

3. The film material must not be amplifying.

These condition are met for most practical application of ellipsometry.

2.3.1 The Equation of Reflection Ellipsometry for Ambient-Film-Substrate System

For application of reflection ellipsometry, the model of an ideal optically isotropic three phase ambient film substrate system is adequate. To this system the complex

reflection coefficients ρ is defined as

$$\rho = \frac{R_p}{R_s} = \frac{r_{01p} + r_{12p} \exp -i2\beta}{1 + r_{01p} r_{12p} \exp -i2\beta} * \frac{1 + r_{01s} r_{12s} \exp -i2\beta}{r_{01s} + r_{12s} \exp -i2\beta} = \tan \Psi \exp i\Delta \qquad (2.3.17)$$

From the above formula , we can see that ρ depends on the n_0, n_1, n_2, d, ϕ_0 and λ.The the functional dependance of the ellipsometric quantities Ψ and Δ on the system parameter can be symbolically written as

$$\tan \Psi \exp i\Delta = \rho(n_0, n_1, n_2, d, \phi_0, \lambda) \qquad (2.3.18)$$

This may be broken into two real equation for Ψ and Δ as

$$\Psi = \arctan \mid \rho(n_0, n_1, n_2, d, \phi_0, \lambda) \mid$$

$$\Delta = \arg \mid \rho(n_0, n_1, n_2, d, \phi_0, \lambda) \mid \qquad (2.3.19)$$

Where $\mid \rho \mid$and arg $\mid \rho \mid$are absolute value and argument (angle) of the complex function of ρ respectively. Equation (2.3.19) is quite complicated, therefore, there is need of iteration which is easily handle using computer.

2.4 Types of Ellipsometry

Depending on how the ellipsometry is arranged and optical component used, there are different types of ellipsometry. The two major broad division are null and photometric ellipsometry.

2.4.1 Null Ellipsometry

In the first ellipsometers, the operator observed the light beam that was reflected off the sample through an eyepiece. The polarizers and retarders were rotated by

hand until the effect of the polarization was inverted and no light would pass through the instrument. This is called the nulling technique. Modern nulling ellipsometers use computers to rotate the elements and to automatically calculate the ellipsometry signal very quickly. However, the nulling technique is not ideal for automated instruments because it is based on measuring a zero signal. This was an advantage in the early ellipsometers because the human eye is very sensitive to small changes in the signal around the 'null'. However, modern light detectors exhibit significantly higher noise at low intensities. Null ellipsometry based on finding a set of azimuth angles for the polarizer, compensator and analyzer (P, C, A) such that the light falls on the photodetector is extinguished. If the variable retardation-compensator is used, beside the three azimuth angles P, C and A, the relative retardation δ_c of the compensator is the fourth parameters that can be adjusted in search for null condition [21].

2.4.2 Photometric Ellipsometry

Photometric ellipsometry is based on utilization of the variation of the detected light flux as a function of one or more of the azimuthal angle, phase retardation or the incident angle ϕ_0. Based on how these quantities (azimuthal angle, phase retardation or the incident angle ϕ_0) measured, there are two types of photometric ellipsometery. These are:

1. Static Photometric Ellipsometry

In this case, the the detected signal (usually dc unless a chopper is used to interrupt the source beam) is recorded at predetermined fixed setting of ellipsometric components, i.e at a specific value of azimuthal angle, phase retardation or the incident

angle ϕ_0 (P, C, A and δ_c)

2. Dynamic Photometric Ellipsometry

In the case of dynamic photometric ellipsometer, one or more of the optical parameters P, C , A and δ_c is periodically varied with time and the detected signal is Fourier analyzed. Depending on the optical components used for modulation there are different types of dynamic photometric ellipsometry. If the linear polarizer is used, rotating analyzer (RAE) and rotating polarizer (RPE). If a retarder is used, rotating compositor (RCE) and the phase modulation ellipsometry (PME) and so on. But in this paper we limit ourselves to the rotating analyzer ellipsometer(RAE) that is preferable and suitable for this work [14].

2.5 Rotating Analyzer Ellipsometry (RAE)

The arrangements of the optical components of rotating analyzer ellipsometer are either the polarizer compensator system analyzer (PCSA) or polarizer system compensator analyzer (PSCA) sequences can be used. The compensator is not associated here[18, 19], so that the polarizer system analyzer (PSA) [14] sequence is used with the other elements (P, C) with a fixed azimuthal angle. The analyzer is constantly rotated with a constant angular speed around the beam axis and the detector signal I_D is Fourier analyzed.

2.5.1 Ellipsometry Equation for RAE

In the perfect RAE setting a laser beam (L) from the laser source pass through the fixed polarizer before touching the surface of the sample. This produce linearly polarized light that can be decomposed in to two linearly polarized components, one in the plane of incident ($E_p^{'}$) and the one perpendicular to it ($E_s^{'}$), having the same phase. After reflection from the sample the recombined light is elliptically polarized. The light ellipse is described basically by the two numbers, its orientation with respect to the plane of incident and the ratio of the two principal axis. These two parameters are measured by the two remaining parts, analyzer and detector.

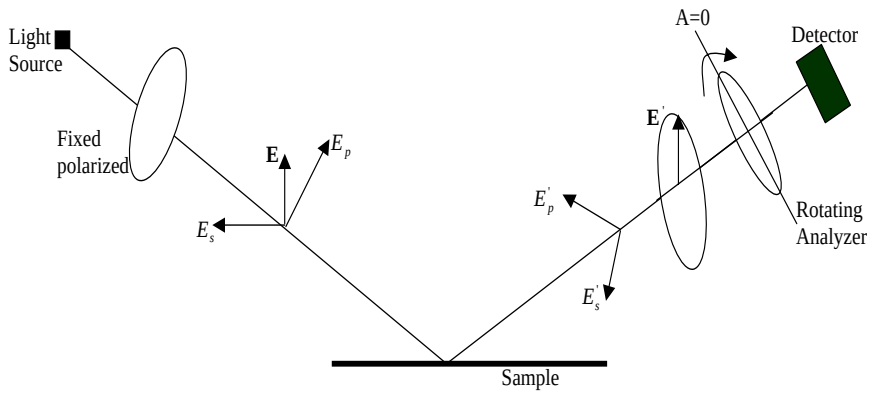

Figure 2.2: The principle of a Rotating Analyzer Ellipsometer.

Let $L, M_p, SandM_A$ are the Mueller matrices of source, polarizer, sample and analyzer respectively, and $R(-p), R(p)$ are rotational matrices. The laser beam passing through a polarizer at azimuthal angle p must be multiplied by a matrices

$$R(-p) \times M_p \times R(p) \times L$$

and after interaction with the sample, the laser beam must multipled by the Mueller matrix of the sample under study, and then after it passed through the analyzer. It must also be multiplied with a Mueller matrix of the analyzer. Finally on the detector the field amplitude is the following

$$E_d = M_A \times R(-p) \times E^{'} \times M_p \times R(p) \times L \tag{2.5.1}$$

The intensity I_D seen by the detector can be expressed by

$$I_D = (1 - \cos 2\Psi \cos 2p)\left[1 + \cos 2A \frac{\cos 2p - \cos 2\Psi}{1 - \cos 2\Psi \cos 2p} + \sin 2A \frac{\cos \Delta \sin 2\Psi \sin 2P}{1 - \cos 2\Psi \cos 2p}\right] \tag{2.5.2}$$

By rotating the analyzer, we can measure the intensity on the detector as a function of analyzer angle A. Because of the ellipse of the light, it has a sinusoidal form

$$I_D = g(1 + a \cos 2A + b \sin 2A) \tag{2.5.3}$$

Where

$$g = 1 - \cos 2\Psi \cos 2p$$

$$a = \frac{\cos 2p - \cos 2\Psi}{1 - \cos 2\Psi \cos 2p}$$

and

$$b = \frac{\cos \Delta \sin 2\Psi \sin 2P}{1 - \cos 2\Psi \cos 2p}$$

where P is the angle of the first polarizer which is kept fixed during measurement. The coefficient a and b do not depend on the intensity of the source, so that there is no need of reference measurement for the intensity. Using the above equation the ellipsometric parameters Δ and Ψ can be expressed explicitly as a Fourier coefficient a and b of this harmonic function as

$$\cos 2\Psi = \frac{\cos 2p + a}{1 + a \cos 2p} \quad and \quad \cos \Delta = \frac{-b}{\sqrt{1 - a^2}} \frac{\sin 2p}{\mid \sin 2p \mid} \tag{2.5.4}$$

When the transmission axis of the polarizer is set an angle 45^0 with the plane of incident, and the starting position of the transmission axis of analyzer is in the plane of incident, equation (2.5.4) became

$$\cos 2\Psi = a \quad and \quad \cos\Delta = \frac{-b}{\sqrt{1-a^2}} \tag{2.5.5}$$

The value of a and b can be obtained by fitting the measured curve. After this the only thing left is to correlate them to the properties of the sample. Therefore, the ellipsometric quantities Δ and Ψ that characterize the sample under investigation are easily computed using equation (2.5.5).

2.5.2 Multiple-Angle-of-Incidence Ellipsometry (MAI)

For a given ambient film substrate system, all are assumed to be homogeneous and optically isotropic, measurement of the ratio of reflection coefficient ρ at one wave length λ and one angle of incident ϕ_0 provide enough information to determine two real optical parameters of a system only assuming that all remaining parameters are known. When a number of unknown optical parameter of the three phase system exceed two, it is necessarily to get additional experimental data to determine such a parameters. In most general case, all the seven parameters, film thickness d, real and imaginary parts of the three complex refractive index of n_0, n_1, n_2 of the three phases, may all be measured. There are different methods of increasing the numbers of ellipsometric measurement, but the one that we use is multiple-angle-of-incidence (MAI)[21]. In this case, measurements of the ratio of reflection coefficient ρ at an adequate numbers of properly chosen angle of incident provide enough information to determine all the optical parameters of a given ambient film substrate system,

without perturbing the system in any manner. MAI is powerful and advantageous method due to its simplicity and non-destructive nature.

Chapter 3

Instrumentation And Measuremental Procedure

3.1 Nature of Sample And Its Preparation

The sample used on this experiment is APFO-Green6. These polymer use in plastic solar cells. It is an alternating polyfluorene copolymer,and is formed from poly[2, n7-(9,9-dioctyl-fluorene)-alt-5, 5-(4', 7'-di-2-thienyl-2', 1', 3-benzo-thiadiazole)], and its blends with the fullerene derivative [6,6]-phenyl-C61-butyric acid methyl ester [11]. Its chemical stricture is given below. The incorporated fluorene units alternating with groups including electron-withdrawing (A) and electron-donating (D) groups in donor-acceptor-donor (DAD) sequence to achieve the lowering of band gaps. The HOMO-LUMO values were estimated from electrochemical studies. By varying the donor and acceptor strength and position of the solubilizing substituents, similar HOMO values were obtained. These values were also found to correlate well with the open circuit voltage (VOC) values determined from photovoltaic data of the

polymers blended with the acceptor PCBM. Despite similar HOMO values, the absorption spectra of the polymers differ significantly. This prompted the preparation of photovoltaic devices consisting of blends of two polymers with complementary absorptions in combination with PCBM to harvest more photons in the polymer solar cells.

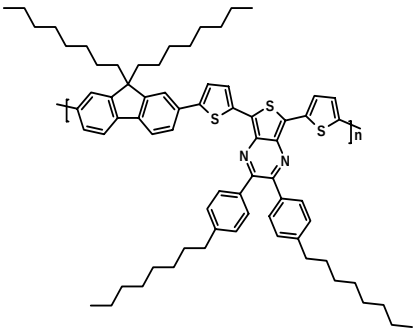

Figure 3.1: Chemical stracture of the polymer APFO-Green6

The film is spin coated on the glass substrate with a speed of 600 rpm. The spinning speed determines the thickness of the film.

3.2 Basic Principle of Operation of RAE

A general scheme of RAE setup is shown in figure 2.2. It can be seen from the figure that a light source, which is well collimated, passes through a polarizer at an azimuthal angle P. The light will be linearly polarized after passing through the polarizer. This linearly polarized light interacts with the sample and its state of polarization is modified due to the interaction. The modified state of polarization of the light is then analyzed by the analyzer. In RAE, by varying the azimuthal angle of

the analyzer A, the induced change of polarization of the light is characterized. The photo detector which is placed after the analyzer detects the light flux after passing all the the optical components. The light detected is then amplified for measurement by the lock in amplifier, which measures the rms of the signal.

3.2.1 Instrumentation of Rotating Analyzer Ellipsometry

In this experiment a specially designed rotating analyzer ellipsometer is assembled for a multiple angle of incidence ellipsometry measurement. Three nano rotators, which are controlled by the stepper motor controllers, are assembled together for this setup. The sample is placed on one of the nano rotators so that the angle of incidence varies as it rotates. The other nano rotator holds the analyzer and detector. As the angle of incidence is varied by rotating the sample, the analyzer and the detector traces the reflected light. This can be achieved by rotating with the speed twice that of the sample. The last nano rotator holds the analyzer. For a given angle of incidence, the analyzer is rotated by 360^0 and the ellipsometric quantities Δ and Ψ are measured. This new RAE ellipsometer has a number of advantages. As the nano rotator has a high degree of accuracy of 0.001^0, the angle of incidence and the azimuthal angle of analyzer are measured more accurately. This is very important since reflection ellipsometry is very sensitive. A relatively small error can lead to a very erroneous results. The other advantage is that multiple angle of incidence measurement can easily be accessed using this setup. Every components are controlled by a computer so that there is no need to manually adjust the different incident angles.

Four laser sources are used in this experiment. The first one is a 5mW He-Ne laser

of wavelength 632.8 nm. The second one is a semiconductor laser of wavelength 660 nm which can give a maximum power of 1mW. The third one is a temperature tunable semiconductor diode laser which has a maximum output power of 450 mW at wavelength 808 nm.The fourth one is the Nd:YAG laser pumped by the semiconductor diode laser and has a maximum power of 100 mW at a wavelength of 1064 nm. Using a KTP crystal the 1064 nm laser in converted to its second harmonic frequency i.e. 532 nm. The light sources are chopped by a chopper. The chopper changes the continuous light signal to a pulsed square wave. The optimum chopper frequency must be set so that the lock-in-amplifier measures only the required signal out of the ambient noise signals. The data acquisition is performed by a lock-in-amplifier which is controlled by a powerful software LabVIEW.

3.2.2 Recommendation

A polarizer imperfection result in a residual ellipticity of the light, that means light leaving the polarizer totally polarized with a small ellipticity. Since the ellipsometric parameters $\Psi$and Δ are susceptible to the error caused by polarizer imperfection, it is advisable to use better optical element.

For many industrial and scientific laser applications it is necessary to have a good laser beam quality. Laser-beam propagation can be approximated by assuming that the laser beam has an ideal Gaussian intensity profile, corresponding to the theoretical TEM_{00} mode. The output from real-life lasers is not truly Gaussian (although helium neon lasers and argon-ion lasers are a very close approximation). In the case of diode pumped Nd:YAG laser (532 nm, 808 nm and 1064 nm) the deviation is very high. Therefore care must be taken to minimize beam divergence and get the Gaussian

beam. For divergent beam, the measured values of Δ and Ψ represents an average over a range of angles of incidence.

From the inter component multiple reflection there is a possibility to arise several out collimated beam (that are folded on the primary forwarding traveling beam), and will find their way to the photo detector. The intensity of these overlapping parasitic rays at the photo detector will depend on the number of multiple reflection that they have experienced, and their polarization states and will affect the results drastically. To avoid these it is advisable to use a small aperture at the telescope or a special filter in front of the photo detector.

3.2.3 Calibration of Rotating Analyzer Ellipsometry

Reliable operation of any ellipsometer stands or fails with the accurate determination of the position of all of its component relative to the plane of incidence. During calibration procedure, the position of all components relative to the plane of incidence to the sample under investigation, are determined. If this step is not taken under careful consideration, the resulting Ψ and Δ spectra are strongly affected. Hence, calibration is very critical step in the experiment.

In calibration, the correct azimuthal angle of the analyzer and the polarizer is sought. Figure 3.2 gives the azimuthal angle of the analyzer versus the intensity of the reflected light for the glass substrate. The polarizer is set at 0^0 i.e. the incident light is s-polarized. The reflected light is also s-polarized. The correct position of the analyzer gives maximum transmission at 0^0 and 180^0, and the minimum transmission at 90^0 and 270^0. This calibration is repeated for a number of times [22].

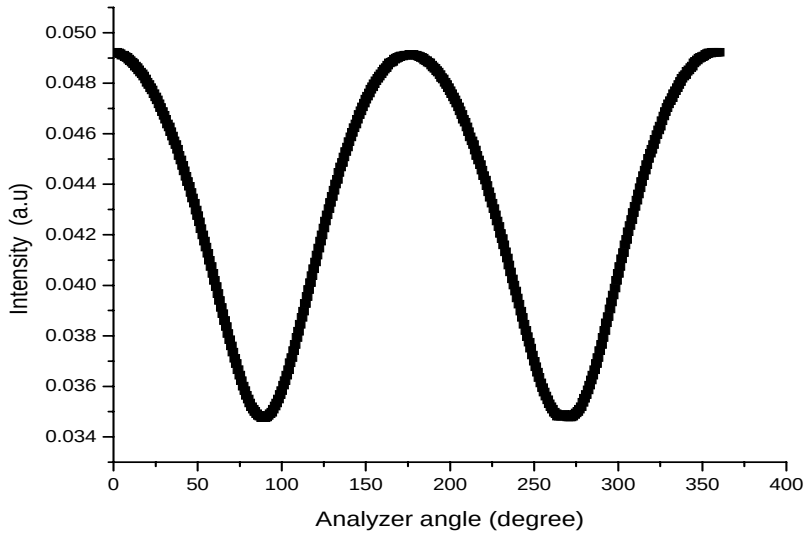

Figure 3.2: Reflected intensity for S-polarized incident light versus analyzer angle for glass.

3.3 Measurement and Procedure

Once the calibration is made, different measurement can be made using reflection or transmission ellipsometry. For a given substrate, the Brewster angle is measured. The procedure for the Brewster angle measurement is given below.

1. Set the polarizer at azimuthal angle P, this angle must be different from 0^0 i.e. the incident light must not be perpendicular to the plane of incidence.

2. Set the analyzer angle at 0^0

3. Rotate the sample. Here the APT (Advanced Positioning Technology) stepper motor controller (Melles Griot)user interface software that controls the stepper motors and the LabVIEW that acquires data from the lock-in-amplifier must run simultaneously.

4. Draw the intensity versus angle of incidence.

The Brewster angle is the angle where the s-component of the reflected light vanishes. Therefore, the angle where the intensity becomes zero or minimum is sought. For glass, the index of refraction can easily be determined from Brewster angle measurement. In the case of a thin film substrate system, the index of refraction, obtained from the Brewster angle, can be used as an initial guess in the simulation programme. The other measurement made is multiple angle of incidence rotating analyzer ellipsometry. For a fixed angle of incidence, the analyzer is rotated through 360^0. The intensity versus the analyzer angle is plotted. The Fourier coefficient is obtained by fitting the curve and the ellipsometric quantities Δ and Ψ are computed. This is repeated for different angles of incidence and wavelengths.

Chapter 4

Results, Analysis and Discussion

4.1 Numerical Inversion for Ellipsometric Data

The Fresnel reflection and transmission coefficients at 0-1 and 1-2 interface of the ambient-film-substrate three phase system that appears in equation (2.3.8) to (2.3.15) can be written as

$$r_{01p} = \frac{\cos\phi_0 - \frac{\cos\phi_1}{n_1}}{\cos\phi_0 + \frac{\cos\phi_1}{n_1}} \tag{4.1.1}$$

$$r_{12p} = \frac{\frac{\cos\phi_1}{n_1} - \frac{\cos\phi_2}{n_2}}{\frac{\cos\phi_1}{n_1} - \frac{\cos\phi_2}{n_2}} \tag{4.1.2}$$

$$r_{01s} = \frac{\cos\phi_0 - n_1\cos\phi_1}{\cos\phi_0 + n_1\cos\phi_1} \tag{4.1.3}$$

$$r_{12s} = \frac{n_1\cos\phi_1 - n_2\cos\phi_2}{n_1\cos\phi_1 + n_2\cos\phi_2} \tag{4.1.4}$$

for air $n_0 = 1$ and $n_1 = n_f + ik$ and $n_2 = n_s$ (real refractive index of the glass) using snell's law

$$n_s\cos\phi_2 = \sqrt{n_s^2 - \sin\phi_0^2} = N_6, n_1\cos\phi_1 = \sqrt{n_1^2 - \sin\phi_0} = \tag{4.1.5}$$

$$\frac{\cos\phi_2}{n_1} = \sqrt{\frac{n_s^2 - \sin\phi_0^2}{n_s^2}} = \frac{N_6}{n_s^2} = N_8 \tag{4.1.6}$$

$$\frac{\cos\phi_1}{N_1} = \sqrt{\frac{N_1^2 - \sin\phi_0^2}{N_1^2}} = \frac{N_7}{N_1^2} = N_9 \tag{4.1.7}$$

Recalling the equation of phase shift, i.e equation (2.3.1)

$$\beta = \frac{2\pi d n_1 \cos\phi_1}{\lambda} = \frac{2\pi d\sqrt{n_1^2 - \sin\phi_0^2}}{\lambda} \tag{4.1.8}$$

$$-2\beta = -4\pi(\frac{d}{\lambda})\sqrt{n_1^2 - \sin\phi_0^2} = \frac{-4\pi d N_7}{\lambda} = N_0 \tag{4.1.9}$$

substituting equation (4.1.5-4.1.9) in equation (4.1.1-4.1.4) gives

$$r_{01p} = \frac{\cos\phi_0 - N_5}{\cos\phi_0 + N_5} \qquad r_{12p} = \frac{n_5 - n_4}{n_5 + n_4} \tag{4.1.10}$$

$$r_{01s} = \frac{\cos\phi_0 - N_7}{\cos\phi_0 + N_7} \qquad r_{12s} = \frac{n_7 - n_6}{n_7 + n_6} \tag{4.1.11}$$

The reflection coefficient can be rewrite as

$$\rho = \rho_1 + i\rho_2 \tag{4.1.12}$$

using this, we find that

$$\psi = a\tan\sqrt{\rho_1^2 + \rho_2^2} \tag{4.1.13}$$

$$\Delta = arg(\rho) = a\tan(\frac{\rho_2}{\rho_1}) \tag{4.1.14}$$

Since the equation is not convergent, we need to have some other means to get the required values. To do so numerical method is applied using the programme written in Visual C sharp. The complete programme can be found in the appendix chapter of this thesis.

4.2 Choice of Error Function for Ellipsometric Data

Since the number of unknown optical parameters for the three phase system exceed two, photometric measurement of reflectance and transmittance intensity for several wavelength may provide an additional data.

let ρ_i^m denote the ratio of reflection coefficient from the i^{th} measurement for an ambient-film-substrate system, and ρ_i^c be the computed value of this ratio. The computational problem in reflection ellipsometry consists of the search for a set of optical parameters (n_s, n_f, k_f, d) that characterize the optical system under measurement such that the quantity

$$F = \sum_{i=1}^{m} \mid \rho_i^m - \rho_i^c(n_s, n_f, k_f, d, \phi_0, \lambda) \mid^2, \tag{4.2.1}$$

is zero or minimum. Where m is the number of measurements. Depending upon which procedure is used to secure additional measurements, any one or a combination of optical parameters (n_s, n_f, k_f, d or ϕ_0) can be different from one measurement to the next one.

Let the multiple-angle-of-incident (MAI) measurement can be made at m different angle of incident ϕ_{0i} from equation (2.3.18) and (2.3.19) $2m$ simultaneous non-linear equation are obtained that relate the measured ellipsometric quantities ψ_i^m and Δ_i^m at a given wavelength to the optical parameters n_s, k_s, n_f, k_f and d of the film and substrate system as

$$\begin{aligned} \Psi_i^m &= \psi_i^c(n_s, k_s, n_f, k_f, d, \phi_{oi}) \\ \Delta_i^m &= \Delta_i^c(n_s, k_s, n_f, k_f, d, \phi_{oi}) \end{aligned} \tag{4.2.2}$$

Where $i = 1, 2, 3.....M$ and the superscript m and c distinguish the measured and computed values of Ψ and Δ respectively. In ideal situation where there are no experimental or model error, it should be possible to compute the value for the unknown optical parameters that should make F identically zero. However, instrumental and model imperfection are available F has to be minimized by numerical computation.

The error function that may be chosen is not unique and the forms of equation (4.2.1) represents only one possibility. Based on dealing with Ψ and Δ directly and not ρ, an alternate error function G can be defined as

$$G(\mathbf{B}) = \sum_{i=1}^{m} (\Delta_i^c(\mathbf{B}) - \Delta_i^m)^2 + (\Psi_i^c(\mathbf{B}) - \Psi_i^m)^2, \tag{4.2.3}$$

If the parameter n_s, k_s, n_f, k_f and d are represented as a component of a vector $\overrightarrow{B} = (b_1, b_2, b_3....)$ which characterize the sample under study, the computational parts of the problem is find a vector B_0, such that $G(B)$ is minimum or zero. The computational problem is certainly dependant on the error function. Since the weighting involved in the error function F is unwarranted, it is preferable to use the error function $G(B)$ for computational numerical inversion approach.

4.2.1 Condition for Simulation

For a three phase (ambient-film-substrate) system to be able to simulate and fit Ψ and Δ spectra obtained in RAE, the following main features is assumed.

- A layer system is defined as a semi-infinite substrate , one layer of definite thickness and semi-infinite ambient.
- For substrate and the film , the refractive index can be definite at fixed value.
- Simulation and fits can be done as function of angle of incidence for each wavelength.
- In fitting the refractive index and the thickness, the strength are determined by minimizing the sum of the square of difference between measured and calculated values of Δ and Ψ.

4.3 Parameters Correlation Test

Using numerical inversion may face a problem that the m measurements might not give independent equations. In this case two or more parameters are correlated. The correlation between two parameters b_j and b_k occur if

$$\frac{\partial Y}{\partial b_j} = c\frac{\partial Y}{\partial b_k}$$

where c is a constant over the range of angles measured. Here Y represents either Δ or Ψ. If measurement is made at m-angles of incidence giving 2m data points (Δ and Ψ), 2m optical parameters can be determined. Mathematically, correlation reduces the number of independent equationss to less than $2m$.

Angle of incident(deg)	$(\frac{\partial\Delta/\partial d}{\partial\Delta/\partial n_f})$	$(\frac{\partial\Delta/\partial d}{\partial\Delta/\partial k_f})$	$(\frac{\partial\Delta/\partial n_s}{\partial\Delta/\partial n_f})$	$(\frac{\partial\Delta/\partial n_f}{\partial\Delta/\partial k_f})$
54.5	0.0115	0.0002	0.7188	0.0239
56.5	0.0174	0.0003	0.7688	0.0172
58.5	0.0102	0.0002	0.7774	0.0261
60.5	0.0119	0.0011	0.0994	0.0853
62.5	0.0272	0.0016	0.3185	0.0591

Table 4.1: Test for correlation of the optical parameters for APFO-Green6 at 1064nm

The correlation test is performed taking the partial derivative of Δ or Ψ by varying one parameter and keeping the others constant. For five angles of incidence, the derivatives vary for wavelength 1064nm (see Table (4.1)). Hence, the four optical parameters (n_s, n_f, k_f, and d_f) are uncorrelated for APFO-Green6. Combining data at multiple angle of incidence at several wavelengths avoids the correlation of the parameters. This reduces the interdependence of the parameters and allows ellipsometry to determine more optical information. The uncertainty in the optical uncorrelated

parameter b_j is calculated using the following relation.

$$\delta b_j = (\frac{2\delta G}{\partial^2 G/\partial b_j^2})^{\frac{1}{2}} \tag{4.3.1}$$

b_j can represent real refractive index, imaginary refractive index of the film or substrate or the thickness of the film. δG is the uncertainty of error function G. This results from the errors in the measured and simulated ellipsometric quantities Δ and Ψ. The denominator is a second partial derivative of the error function. Since error in the Fourier coefficients of the detected signal is known, the errors in the measured Δ and Ψ can easily be calculated from Taylor expansion.

$$\delta\Psi^m = \frac{\delta a}{2\sqrt{1-a^2}}$$

$$\delta\Delta^m = \frac{\sqrt{((1-a^2)\delta b)^2 + (ab\delta a)^2}}{1-a^2\sqrt{1-a^2-b^2}}$$

The uncertainty in G (δG) is calculated from the above uncertainties for each angle of incidence.

4.4 Data from the Absorption Spectrum

The electric field wave propagates through a material medium of a refractive index $n(\omega) = n_R(\omega) + n_I(\omega)$ is given by

$$\overrightarrow{E}(z,t) = E_0 e^{\frac{-n_I(\omega)\omega z}{c}}.e^{-i\frac{\omega t - n_R(\omega)\omega z}{c}} \tag{4.4.1}$$

The the above equation shows that $\overrightarrow{E}(z,t)$ is not purely oscillatory due to $n_I(\omega)$. The field decay with increasing distance of propagation. Since the intensity is proportional to the electric field. The intensity is given as

$$I_\omega(z) \propto \overrightarrow{E}^2 = I_\omega(0)e^{-a(\omega)\omega z} \tag{4.4.2}$$

Where $a(\omega)$ is the absorption or extinction coefficient which can be given as

$$a(\omega) = \frac{2n_I(\omega)\omega}{c} \tag{4.4.3}$$

here, it is possible to show how the absorption coefficient depends on the wavelength λ of the light. i,e

$$a(\lambda) = \frac{4\pi n_I}{\lambda} \tag{4.4.4}$$

Therefore we can understand that the case of absorption is due to the complex parts of the refractive index of the material. This implies as the wave propagates, the energy is absorbed by the material. The transmitted intensity is proportional to $\mid \overrightarrow{E} \mid^2$. Transmittance T is defined as the ratio of transmitted intensity to initial intensity.

$$T = \frac{I_t}{I_0} = e^{-az}$$

If we take the negative logarithm of transmission, we get the absorbance of the material.

$$A = \frac{4\pi kd}{ln(10)\lambda}, \tag{4.4.5}$$

Where λ is wavelength k is extinction coefficient of the material and d is thickness of the material

The absorbance of the polymer APFO-Green6 is obtained from UV/Vis spectrometer. It has a peak value at wavelength around 400 nm and 760 nm. At these two particular wavelengths, the sample is highly absorbing. The absorbance decreases rapidly as the wavelength increases towards the right of the peak in the visible range till the wavelength 540nm that it attain the minimum absorption. After this point

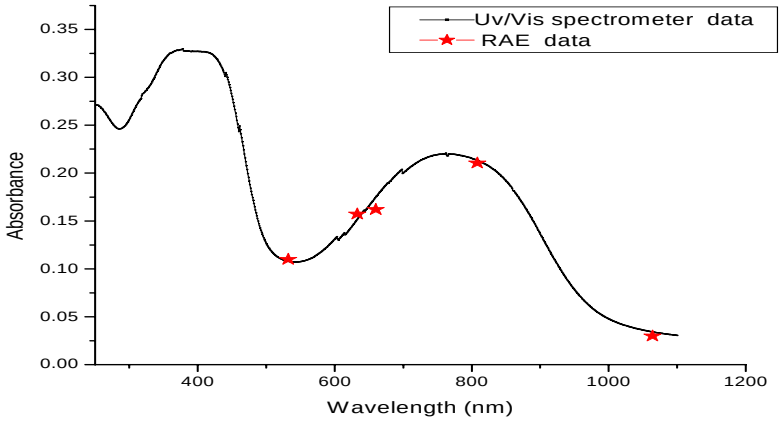

Figure 4.1: The two independent measurement of Absorbance of APFO-Green6

the polymer absorption increase until it reach the second peak of absorption. The absorption of the APFO-GReen6 decrease as it the wave length increase in the IR region as shown in the figure (4.1). Around the wavelength 540 nm and above 760 nm the polymer is almost transparent with small value of absorbance.

4.5 Data from Brewster Angle Measurement

Theoretically at Brewster angle the reflected intensity of the electric field (light) parallel to the plane became zero or minimum. To observe this the transmissions axis of the incident analyzer lies along the plane of incident, and the intensity of the reflected light for both the glass substrate and the ambient film substrate to all wavelength that used in the experiment is recorded as a function of angle of incident.

The brewster angle of the glass substrate are 57.6^0, 57^0, 56.8^0, 56.5^0, 56.1^0 and

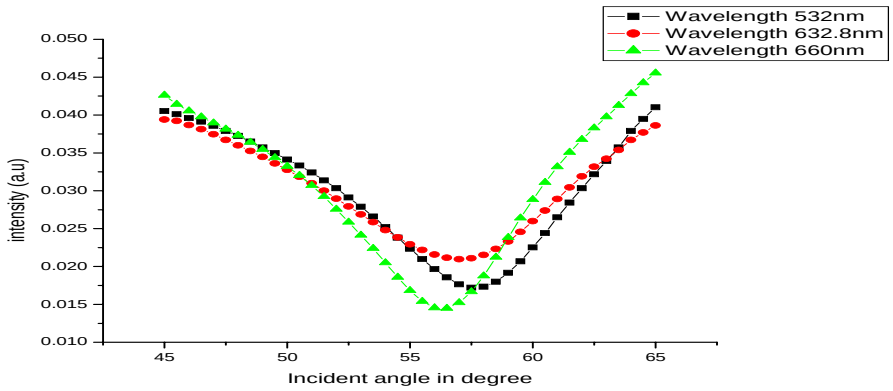

Figure 4.2: Reflected intensity (R_p) versus angle of incidence (θ_0) for glass-substrate

The ambient film substrate are 62^0, 61.5^0, 61^0, 60^0, and 58.5^0 for wavelength 532 nm, 632.8 nm, 660 nm, 808 nm and 1064 nm respectively. Using Brewster angle θ_B and equation

$$n = tan(\theta_B) \tag{4.5.1}$$

The index of refraction of glass substrate and the ambient-film-substrate can be calculated. These values can be used for the initial guesses that feed to the programme for iteration. The other measurement of the reflected light intensity for the ambient-film-substrate are made at a multiple angle of incident which are around the Brewster angle. For a fixed angle incident the analyzer is rotated 360^0. In this case the polarizer set at 45^0. The intensity verses the analyzer angle is plotted. This is done for five different wavelength and five different incident angle for each wavelength. This result is fitted with a user defined equation (2.5.3). From the best fitting the Fourier coefficient a and b are obtained. From these Fourier coefficient the ellipsometric parameters Δ^m and Ψ^m are calculated using equation (2.5.5) for the five angle of

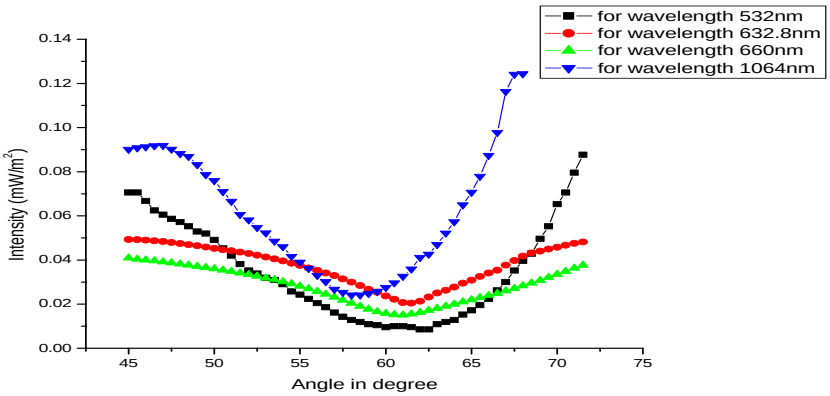

Figure 4.3: Reflected intensity (R_p) versus angle of incidence (θ_0) for ambient-film-substrate

incident to each of the five wavelength.

After these ellipsometric parameters Δ^c and Ψ^c which can give the minimum error G are computed. Then finally both the real and imaginary refractive index, thickness, extinction coefficient and absorbance of the film are calculated. The results are summarized on the Table (4.3).

In the case of absorption of the film there are two independent measurements, one from RAE and the other from UV/VIs spectrometer. Since the thickness and extinction coefficient of the polymer are determined from multiple angle of incidence ellipsometry, the absorbance at a fixed wavelength can be calculated. The two experimental results are compared. It can be seen from in figure (4.1) that the two independent measurements of absorbance are in excellent agreement. The slight difference arises from errors in calculating the extinction coefficient and thickness of the polymer.

4.6 Results for Optical Parameters of APFO-Green6

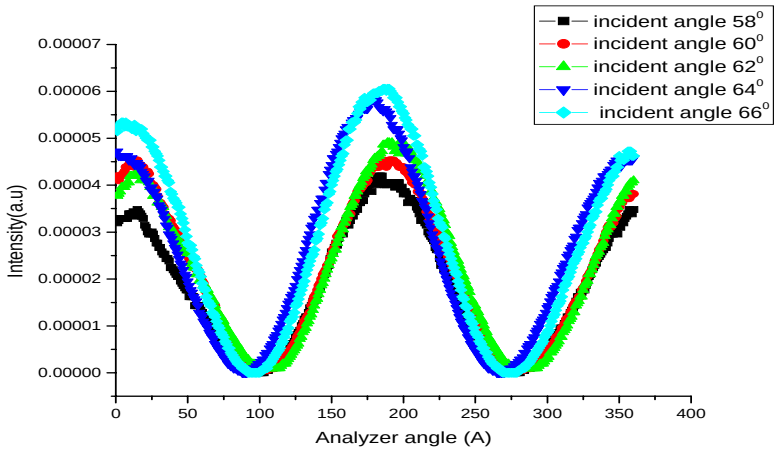

Figure 4.4: Intensity versus analyzer angle for five angles of incidence at wavelength 532 nm.

The intensity wave forms obtained from ellipsometric measurement are sinusoidal in nature and are given by equation (2.5.3). The intensity versus analyzer angle from RAE measurements for five wavelength are plotted (see figure 4.4, 4.5, 4.6, 4.7 and 4.8). The measured reflected intensity versus the analyzer angle is fitted with user defined equation (2.5.3) so that the Fourier coefficients a and b for the best fit are obtained. From Fourier coefficient a and b, the ellipsometric quantities Δ^m and Ψ^m are calculated for five angle of incidence. The simulated Δ^c and Ψ^c that give minimum error function G are sought using the numerical inversion method written in Visual c sharp programme. The measured ellipsometric quantities for five wavelength is presented in table (4.2). Thus, the complex refraction of the APFO-Green6 film,

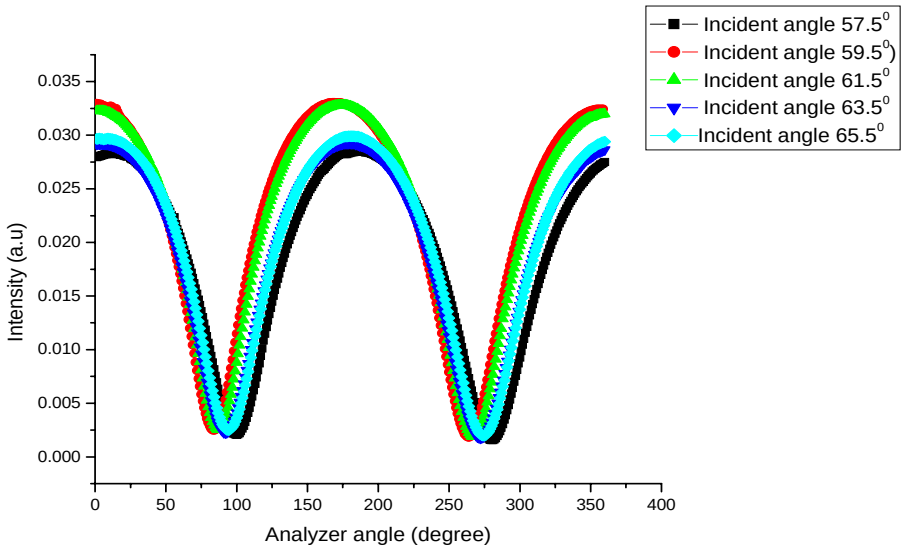

Figure 4.5: Intensity versus analyzer angle for five angles of incidence at wavelength 632.8 nm.

index of refraction of the glass and thickness of the film are obtained. The results are summarized in Table (4.3).

Wavelength(nm)	incident angle (deg)	a	b	ψ^m	Δ^m	δa	δb
	58.0000	0.9707	0.2212	6.9496	157.0501	0.0113	0.0095
	60.0000	0.9155	0.3881	11.8623	164.7158	0.0057	0.0050
	62.0000	0.8901	0.4352	13.5552	162.7250	0.0093	0.0083
	64.0000	0.9518	0.2597	8.9299	147.8746	0.0010	0.0084
532	66.0000	0.9835	0.1782	5.2097	170.1541	0.0094	0.0078
	57.5000	0.9821	-0.0597	5.4255	71.5014	0.0093	0.0091
	59.5000	0.9434	0.3255	9.6856	168.8995	0.0010	0.0099
	61.5000	0.8842	0.4572	13.9246	168.1435	0.0097	0.0096
	63.5000	0.9431	0.2999	9.7080	154.4396	0.0090	0.0089
632.8	65.5000	0.9824	0.1812	5.3781	166.1432	0.0088	0.0088
	57.0000	0.9878	0.0970	4.4887	128.4156	0.0086	0.0091
	59.0000	0.9152	0.3899	11.8822	165.3579	0.0099	0.0055
	61.0000	0.8795	0.4694	14.2108	170.5023	0.0059	0.0028
	63.0000	0.9558	0.2798	8.5454	162.2007	0.0029	0.0057
660	65.0000	0.9927	-0.0544	3.4541	63.1256	0.0091	0.0085
	56.0000	0.9543	0.2903	8.6914	166.3449	0.0034	0.0030
	58.0000	0.9450	0.2994	9.5473	156.2439	0.0018	0.0018
	60.0000	0.8343	0.5508	16.7295	177.4151	0.0013	0.0023
	62.0000	0.9333	0.3516	10.5264	168.1641	0.0014	0.0028
808	64.0000	0.9862	-0.1351	4.7631	35.2939	0.0028	0.0028
	54.5000	0.9026	0.4289	12.7523	174.8844	0.0012	0.0016
	56.5000	0.8867	0.4617	13.7711	176.7961	0.0017	0.0015
	58.5000	0.8392	0.5425	16.4727	175.9051	0.0016	0.0026
	60.5000	0.9626	0.2572	7.8639	161.5862	0.0017	0.0026
1064	62.5000	0.9775	0.2042	6.0872	165.5742	0.0026	0.0032

Table 4.2: Measured ellipsometric parametric quantities from Fourier coefficient obtained from curve fitting.

wavelength	n_f	k_f	n_s	d (nm)	A
532nm	1.7768 ±0.0004	0.11134±0.0005	1.5857±0.0003	97±2	0.1099 ±0.0003
632.8nm	1.8182±0.0004	0.18552±0.0001	1.5498±0.0002	99±1	0.1572±0.0001
660nm	1.8789±0.0003	0.1901±0.0002	1.5381±0.0001	101±1	0.1623±0.0004
808nm	1.7865±0.0005	0.3329±0.0002	1.5308±0.0003	102±1	0.2106±0.0002
1064nm	1.5455±0.0003	0.05763±0.0003	1.5201±0.0001	98±2	0.0299±0.0002
Average				99.4±2.4	

Table 4.3: Measured optical constants and thickness of APFO-Green6 polymer thin film

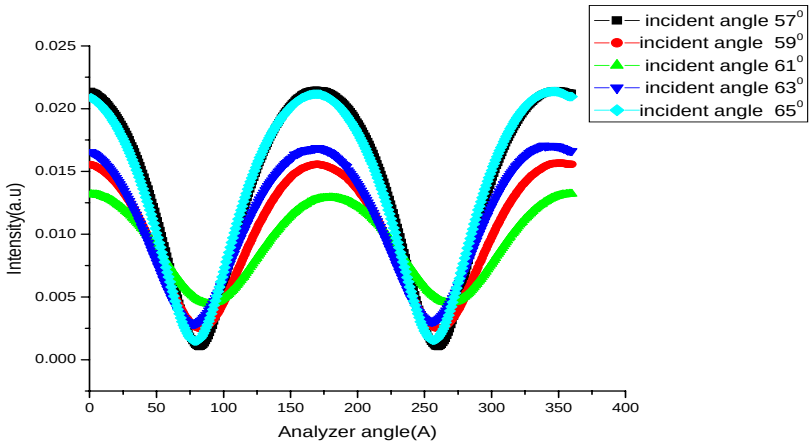

Figure 4.6: Intensity versus analyzer angle for five angles of incidence at wavelength 660 nm.

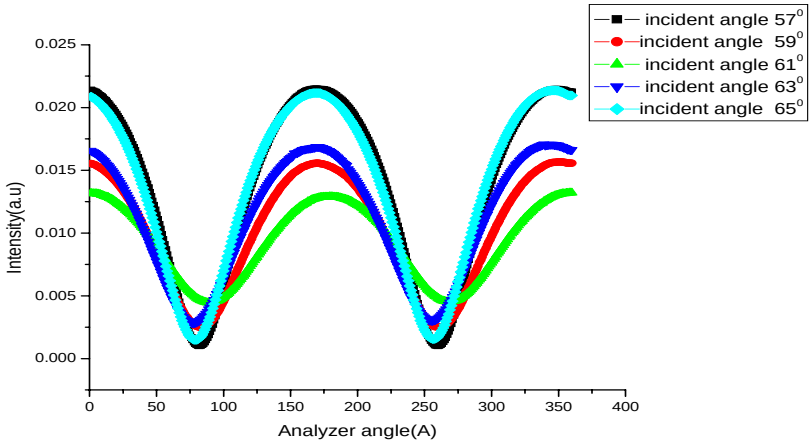

Figure 4.7: Intensity versus analyzer angle for five angles of incidence at wavelength 808 nm.

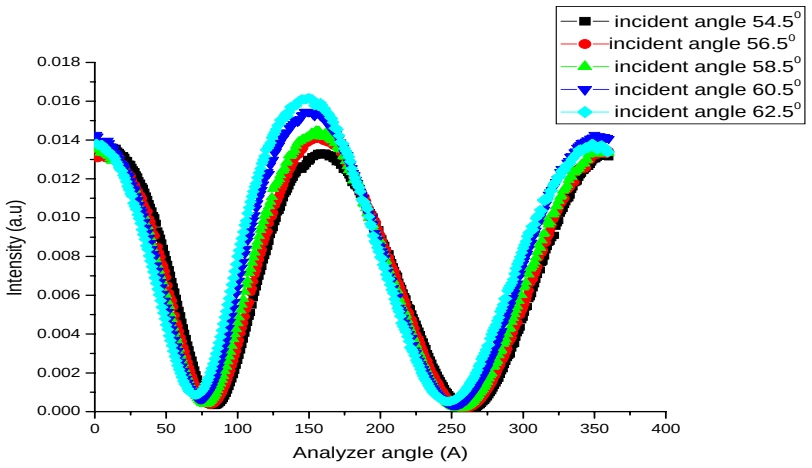

Figure 4.8: Intensity versus analyzer angle for five angles of incidence at wavelength 1064 nm.

Chapter 5

Conclusion

5.1 Conclusion

In this work multiple angle of incidence (MAI) ellipsometry is applied for the determination optical parameters of thin film. The method is based on the measurement of the variation of the polarization state of the light after reflection on a plane surface. The determined parameters include real and imaginary parts of refractive index, and thickness of a material. The index of refraction of the glass substrate was obtained from the Brewster angle measurement. The thickness of the film determined at different wavelengths and remains almost constant with small standard deviation 99.4 $\pm$2.4. This result implies that the optical model fitting is in good agreement with experimentally measured quantities.The real and the complex refractive index of the sample is determined to be 1.7768-i0.1134, 1.8182-i0.1855, 1.8787-i0.1970, 1.7865-i0.3329 and 1.5455-i0.0576 for wavelength 532 nm, 632.8 nm, 660 nm, 808 nm and 1064 nm respectively. The index of refraction is maximum around the wavelength 660 nm, and 808 nm. AS we can see the pattern of the refractive index the dispersion is not normal for wavelength range used in the experiment. It is anomalous dispersion. Further more absorption was measured in two independent measurement, using

UV/VIS spectrometer and MAI ellipsometric measurements, and the values obtained from the two independent measurements are compared. The excellent agreement in the two measurements further strengthens the reliability of the results obtained from MAI ellipsometric measurement.

Appendix

1

1

1

1

1

1

1

1

1

1

Bibliography

[1] B. K. Mathur, Principles of Optics 2^{nd} Ed., John Wiley and Sons, New York, 1986.

[2] M. V. Kleiv and T. E. Furtak, Optics, 2^{nd} Ed., John Wiley and Sons, New York, 1986.

[3] F. L. Pedrotti, Introduction to Optics, 2nd Ed., Englewood Cliffs: Prentice-Hall, 1987.

[4] M. Born and E. Wolf: Principles of Optics, 6^{th}Ed., Cambridge University Press, New York, 1980.

[5] G. R. Fowles, Introduction to Modern Optics, Holt, Rinehart and Winston Inc., New York, 1975.

[6] M. V. Kleiv and T. E. Furtak, Optics 2^{nd}Ed., John Wiley and Sons Inc., New York, 1986.

[7] J. W. Hovenier, Appl. Opt., Vol. 33, 8318-8324, 1994.

[8] U. V. Toussaint, T. Schwarz-Sellinger and C. Hopf, Bayesian Analysis of Ellipsometry Measurements, Max-Planck-Institut fuer Plasmaphysik, Euraton Association, Garching, Germany. 2oo6

[9] A. Hamnett, J. Chem. Soc. Faraday Trans., Vol. 89(11), 1993.

[10] Y. F. Chao, W.-C. Lee, C. S. Hung and J. J. Lin, J. Phys. D: Appl. Phys., Vol. 31, 1998.

[11] W. Mammo, Personal Communication, 2007.

[12] W. A. Bashara and S. S. Shurcliff, Polarized Light, 2nd Ed., Elselvier, Amsterdam, 2003.

[13] S. S. Ballard and W. A. Shurcliff, Polarized Light, Princeton, N.J, 1964.

[14] R. M. A. Azzam and N. M. Bashara, Ellipsometry and Polarized Light, 2^{nd} Ed., Elselvier, Amsterdam, 2003.

[15] R. M. A. Azzam, Ellipsometry in W. L. Wolfe (Ed.), Handbook of Optics, 2^{nd} Ed., Vol. II, McGraw-Hill, New York, 1995.

[16] H. C. van de Hulst, Light Scattering by Small Particles, John Wiley and Sons, New York, 1957.

[17] M. Born and E. Wolf, Principles of Optics, 6^{th}Ed., Cambridge University Press, New York, 1959.

[18] D. E. Aspens, Opt. Comm., Vol. 8, 222, 1973.

[19] P. S. Hauge and F. H. Dill, Opt. Comm., Vol. 14, 431, 1975.

[20] S. N. Jasperson and S. E. Schanatterly, Rev. Sci. Instr. 40, 761, 1969.

[21] T. E. Jenkins, J. Phys. D: Appl. Phys., Vol. 32, 1998.

[22] J. M. M. de Nijs, A. H. M. Holtslag, A. Hoekstra and A. van Silfhout, J. Opt. Soc. Am., 1466, 1988.